

Final States with a Single Charged Particle and Visible Λ from K^-n Interactions at 4.5 GeV/c†

W. L. YEN,*† A. C. AMMANN, D. D. CARMONY, R. L. EISNER,§ A. F. GARFINKEL,
L. J. GUTAY, S. L. KRAMER, AND D. H. MILLER

Department of Physics, Purdue University, Lafayette, Indiana 47907

(Received 18 July 1969)

The results presented in this paper were obtained from an analysis of 372 000 K^-d bubble-chamber pictures at an incident K^- momentum of 4.48 GeV/c. This paper reports the results on two-body final states, such as $\pi^- \Lambda$, $\pi^- \Sigma^0$, $\rho^- \Lambda$, $\pi^- \Sigma^0(1385)$, $\pi^0 \Sigma^-(1385)$, $\pi_N^-(980)\Lambda$, $\eta \Sigma^-(1385)$. The polarization of the Λ hyperon in the reaction $K^-n \rightarrow \pi^- \Lambda$ has been determined and compared with the double-Regge-pole model of Reeder and Sarma. The polarization is large and remains more or less constant. No change in sign was observed, in contrast with the prediction of the model of Reeder and Sarma. A common feature of the observed two-body final states is that their production process is dominated by a peripheral mechanism which arises from meson exchange processes. The exchange mechanism for the reaction $K^-n \rightarrow \rho^- \Lambda$ was investigated in terms of the density matrix formalism. It was found that more than one exchange contributes to the production of this final state. The $\pi_N^-(980)$ meson was observed in the reaction $K^-n \rightarrow \pi_N^- \Lambda$. The decay mode observed was $\pi_N^- \rightarrow \pi^- \eta$. The mass observed is 0.98 ± 0.01 GeV with a width of 0.06 ± 0.03 GeV.

I. INTRODUCTION

IN this paper we present further analysis of K^-d interactions at an incident K^- momentum of 4.48 GeV/c. The data were obtained from a 372 000-picture exposure in the Argonne National Laboratory 30-in. deuterium bubble chamber.

The film was scanned for events of the type two-prong plus V and one-prong plus V . The experimental results presented in this paper are limited to those events in which the V is a Λ .¹ The following hyperon hypotheses were attempted in this analysis:

$$K^-d \rightarrow p_s \pi^- \Lambda, \quad (1)$$

$$p_s \pi^- \Sigma^0, \quad (2)$$

$$p_s \pi^- \Lambda(\pi^0), \quad (3)$$

$$p_s \pi^- \Lambda(MM), \quad (4)$$

$$p_s K^- \Lambda(K^0), \quad (5)$$

$$p_s K^- \Lambda(MM), \quad (6)$$

where the parentheses indicate that the particle is unseen and p_s denotes a spectator proton of momentum less than 300 MeV/c.

A preliminary report based on some of these data has been presented earlier.² The Λ polarization in reaction (1)³ and the production of a $\pi^- \eta$ resonance at a mass of

0.98 GeV in reaction (4)⁴ have been discussed separately.

II. EXPERIMENTAL DETAILS

A. Measurement, Reconstruction, and Kinematic Fitting

The film was scanned twice for events of the types two-prong plus V and one-prong plus V . In the case of the two-prong events, it was demanded that the positive particle be a proton with a momentum less than 300 MeV/c. This was to ensure that the events were predominantly K^- -neutron interactions with the proton being merely a spectator (p_s).

All events of these topologies were measured on three scanning and measuring projectors (SMP) on line to an IBM 360/40-44 system. The geometric reconstruction and kinematic fitting were performed on the IBM 360/40-44 system using the Berkeley programs TVGP-SQUAW.

B. Event Identification

Both the three-constraint Λ and K^0 hypotheses were attempted; if the confidence level of one hypothesis was three times greater than the other, the V was considered as uniquely identified. In this way, 94% of the V 's were uniquely identified. The remaining 6% of the V 's were examined on the scanning table. The majority were found to be Λ 's.

Six hyperon hypotheses represented by reactions (1)–(6) were attempted. In order for a given hypothesis to be considered acceptable, it was necessary that the confidence level for that hypothesis be greater than 1%.

Events with an acceptable fit to reaction (5) in addition usually fitted reaction (3). However, from a study of the two-prong plus two V 's and one-prong

† Work supported in part by the U. S. Atomic Energy Commission.

* A dissertation based on this work has been submitted to Purdue University in partial fulfillment of the requirements for the Ph.D. degree.

† Now at Purdue University, Indianapolis Campus.

§ Now at Brookhaven National Laboratory.

¹ For results in which the V is a K^0 , see R. L. Eisner, Ph.D. thesis, Purdue University, 1968 (unpublished).

² W. L. Yen, A. C. Ammann, D. D. Carmony, A. F. Garfinkel, L. J. Gutay, R. V. Lakshmi, and D. H. Miller, *Bull. Am. Phys. Soc.* **14**, 77 (1969).

³ W. L. Yen, A. C. Ammann, D. D. Carmony, R. L. Eisner, A. F. Garfinkel, L. J. Gutay, R. V. Lakshmi, D. H. Miller, and G. W. Tautfest, *Phys. Rev. Letters* **22**, 963 (1969).

⁴ D. H. Miller, S. L. Kramer, D. D. Carmony, R. L. Eisner, A. F. Garfinkel, L. J. Gutay, and W. L. Yen, *Phys. Letters* **29B**, 255 (1969).

plus two V 's events, only seven events have an acceptable confidence level for the 10-constraint fit:

$$K^-d \rightarrow p_s K^- \Lambda K^0.$$

This corresponds to 14 ± 6 events of reaction (5). Thus reaction (5) and its missing-mass hypothesis (6) will not be considered in the following analysis.

An event was considered uniquely identified if the confidence level of one hypothesis was three times greater than any of the others. The main ambiguities exist between reactions (1) and (2), reactions (2) and (3), and reactions (3) and (4).

The ambiguity between reactions (1) and (2) was resolved by examining the angular distribution of the Λ from Σ^0 decay in the Σ^0 rest frame with respect to the normal (\hat{n}) of the production plane. The distribution should be isotropic for true Σ^0 events. For real Λ events, the Λ is essentially lying on the production plane so that one expects a distribution peaked at $\hat{n} \cdot \hat{\Lambda} = 0$, where $\hat{\Lambda}$ is a unit vector along the Λ direction in the Σ^0 rest frame. The distribution for events whose confidence level for reaction (1) is three times greater than that for reaction (2) is shown in Fig. 1(a). It shows a sharp peak at $\hat{n} \cdot \hat{\Lambda} = 0$ as expected. Figure 1(b) shows the same distribution for the ambiguous events. A peak similar to that in Fig. 1(a) is obvious. Figure 1(c) shows the same distribution for the uniquely identified Σ^0 events. It shows an isotropic distribution. Thus all the ambiguous events were assigned to reaction (1).

The ambiguity between $\Sigma^0\pi^-$ and $\Lambda\pi^-\pi^0$ final states was resolved by examining the effective mass squared

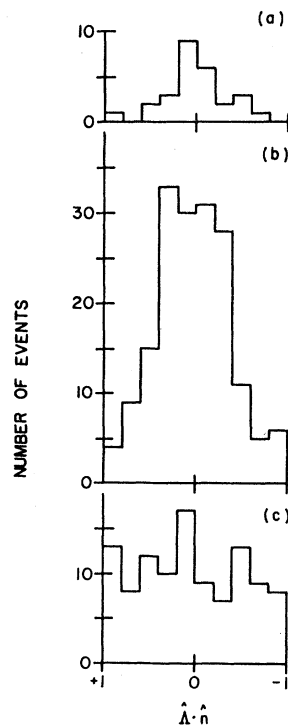


FIG. 1. Angular distribution for Λ from Σ^0 decay: (a) Events whose confidence level for the reaction (1) is three times greater than that for the reaction (2). (b) Ambiguous events. (c) Events whose confidence level for the reaction (2) is three times greater than that for the reaction (1).

of the Λ and missing mass (Fig. 2). This quantity should peak at $M^2(\Sigma^0)$ for true Σ^0 events, while for $\Lambda\pi^0$ events, it should lie above the kinematic threshold of 1.56 GeV^2 . In our analysis the kinematically ambiguous events with $M^2(\Lambda MM)$ less than 1.6 GeV^2 were assigned to the Σ^0 production hypothesis.

Events of reaction (4) might have an acceptable fit to reaction (3). An excess at the right tail of Fig. 3 shows that this is the case. Because of the less stringent

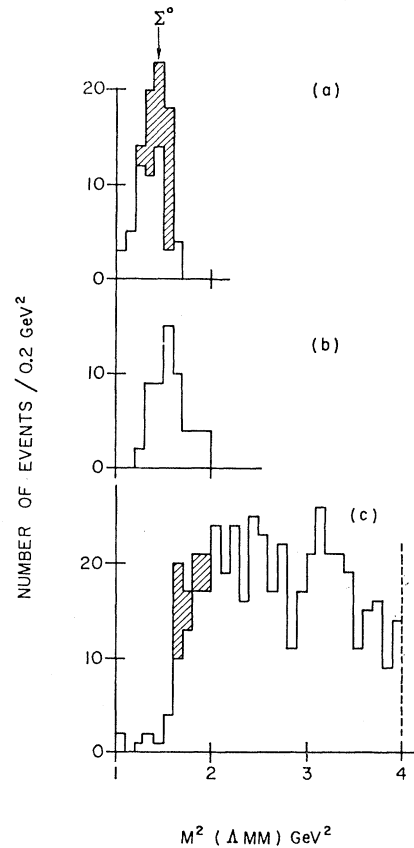


FIG. 2. ΛMM effective-mass distribution: (a) Events whose confidence level for the reaction (2) is three times greater than that for the reaction (3). The shaded area represents the ambiguous events with $M^2(\Lambda MM) < 1.6 \text{ GeV}^2$. (b) Ambiguous events. (c) Events whose confidence level for the reaction (3) is three times greater than that for the reaction (2). The shaded area represents the ambiguous events with $M^2(\Lambda MM) > 1.6 \text{ GeV}^2$.

requirements for a fit to reaction (3), a missing-mass cutoff was imposed. The values chosen were

$$-0.16 < MM^2 < 0.2 \text{ GeV}^2.$$

Using the above criteria, we estimate that the percentages of misassigned events are 5, 20, and 10% for reactions (1), (2), and (3), respectively. The misassignment in events has been taken into account in the cross-section determination. A summary of the number of events accepted for each reaction is shown in Table I.

TABLE I. Number of events accepted for each reaction.

| Reaction channel | Spectator proton | | Total No. |
|----------------------------------|------------------|--------|-----------|
| | Seen | Unseen | |
| $K^-n \rightarrow \pi^- \Lambda$ | 113 | 158 | 271 |
| $\pi^- \Sigma^0$ | 51 | 51 | 102 |
| $\pi^- \Lambda (\pi^0)$ | 332 | 572 | 904 |
| $\pi^- \Lambda (MM)$ | 1052 | 1726 | 2778 |

III. CROSS SECTIONS

The beam purity which was measured by a Čerenkov counter during the entire exposure was 0.98. The total length of K^- beam track contained in our fiducial volume, taking into account the beam purity, was 1.874×10^8 cm. This gives a cross section of $0.140 \mu\text{b}$ for a corrected event.

The cross-section calculation was corrected for scanning efficiency (1.02), Glauber screening effect due to the presence of protons (1.04),^{5,6} neutral decay of Λ (1.53),⁷ losses due to failures in the reconstruction program (1.05), and finite size of the chamber. Each event with an observed decaying Λ was weighted by a factor W ,

$$W = (e^{-l/\eta\tau c} - e^{-L/\eta\tau c})^{-1},$$

where l is the minimum Λ -tracklength cutoff (0.4 cm, see Fig. 4), L is the distance from the production vertex to the boundary of the decay fiducial volume, η is the ratio of Λ momentum to Λ mass, τ is the Λ mean life, and c is the velocity of light. The average value for this factor is 1.11.

Because of vertex problems, the sample with an unseen spectator proton was biased in the very forward

TABLE II. Cross sections.

| Reaction channel | Cross section in μb |
|-----------------------------------|--------------------------------|
| $K^-n \rightarrow \pi^- \Lambda$ | 83 ± 11 |
| $\pi^- \Lambda$ (backward) | 9 ± 3 |
| $\pi^- \Sigma^0$ | 32 ± 10 |
| $\pi^- \Sigma^0$ (backward) | 4 ± 2 |
| $\pi^- \Lambda \pi^0$ (total) | 250 ± 33 |
| $\rho^- \Lambda$ | 70 ± 13 |
| $\rho^- \Lambda$ (backward) | 13 ± 4 |
| $\Sigma^-(1385) \pi^0$ | 16 ± 5 |
| $\Sigma^0(1385) \pi^-$ | 22 ± 8 |
| $\Sigma^-(1610) \pi^0$ | 5 ± 3 |
| $\pi^- \Lambda MM$ (total) | 740 ± 60 |
| $\pi^- \Lambda \eta^a$ (total) | 56 ± 15 |
| $\pi N^- \Lambda^a$ | 15 ± 3 |
| $\Sigma^-(1385) \eta^a$ | 13 ± 4 |
| $\Sigma^-(1610) \eta^a$ | 5 ± 3 |
| $\Sigma^-(1385) MM, MM \neq \eta$ | 60 ± 20 |
| $\Sigma^-(1610) MM, MM \neq \eta$ | 12 ± 5 |

^a The cross sections have been corrected using the neutral branching ratio of the η given in Ref. 7.

⁵ W. Galbraith, E. W. Jenkins, T. F. Kycia, B. A. Leontic, R. H. Phillips, A. L. Reed, and R. Rubinstein, Phys. Rev. **138**, B913 (1965).

⁶ R. Good and N. H. Xuong, Phys. Rev. Letters **14**, 191 (1965).

⁷ N. Barash-Schmidt, A. Barbaro-Galtieri, L. R. Price, A. H. Rosenfeld, Paul Soding, C. G. Wohl, Matts Roos, and G. Conforto, Rev. Mod. Phys. **41**, 109 (1969).

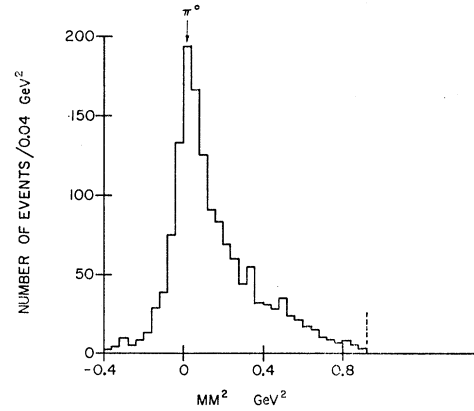


FIG. 3. Missing-mass distribution for the reaction (3).

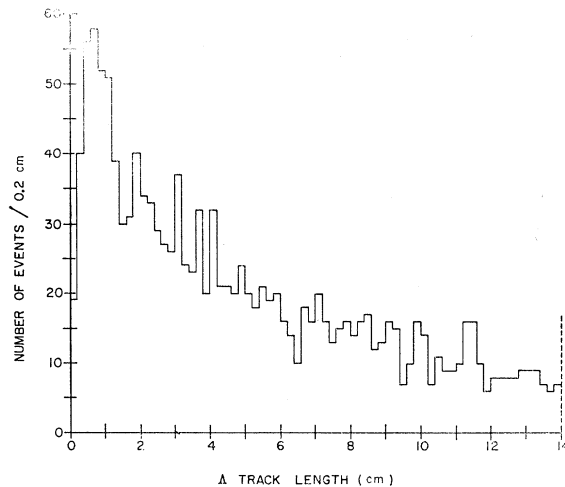
direction. By comparison of the momentum transfer distribution between the sample with a seen spectator proton and the sample with an unseen spectator proton, a correction factor of 1.51 was applied to the events with momentum transfer from the incident K^- to the outgoing π^- less than $0.1 (\text{GeV}/c)^2$.

Because of the cutoff in the spectator momentum at $300 \text{ MeV}/c$, about 2% of the K^-n events were excluded from the analysis.⁸

A summary of the cross sections for the various final states are shown in Table II.

IV. FINAL STATES $p_s \pi^- \Lambda$ AND $p_s \pi^- \Sigma^0$

There were 271 events accepted as being of the type $K^-n \rightarrow \pi^- \Lambda$ and 102 events as $K^-n \rightarrow \pi^- \Sigma^0$. A detailed

FIG. 4. Λ -tracklength distribution.

⁸ L. Hulthén and M. Sugawara, *Handbuch der Physik*, edited by S. Flügge (Springer-Verlag, Berlin, 1957), Vol. 39, p. 1. If the Hulthén wave function is valid, 2% of the spectator protons are expected to have momentum greater than $300 \text{ MeV}/c$. However, in the study of the events with spectator momentum greater than $300 \text{ MeV}/c$, we found that these events might constitute about 10–15% of the total sample.

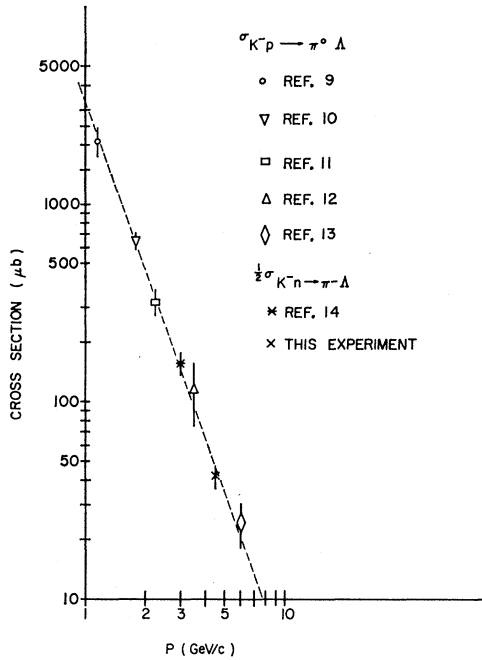


FIG. 5. Cross section as a function of the incident K^- momentum for the reaction $K^-N \rightarrow \pi\Lambda$.

analysis based on part of these samples has already been reported.³ In Ref. 3 the cross sections were overestimated by about 20%. The correct partial cross sections should be 83 ± 11 and $32 \pm 10 \mu\text{b}$, respectively. Since both reaction $K^-n \rightarrow \pi^- \Lambda$ and reaction $K^-p \rightarrow \pi^0 \Lambda$ involve only the pure isospin-1 state, the cross section for the first reaction should be twice that for the second

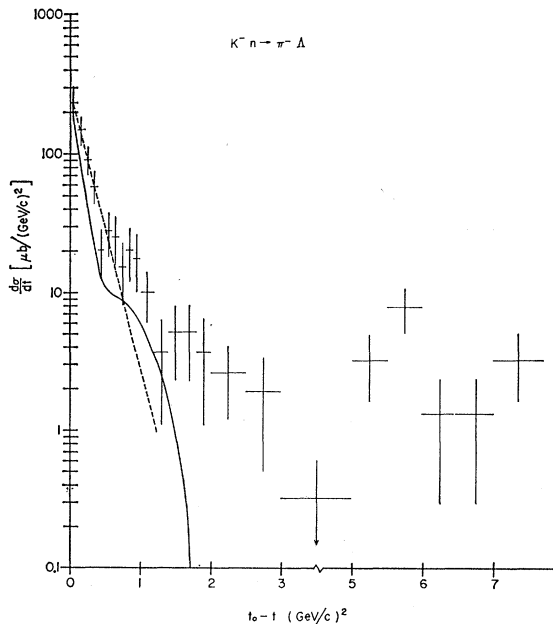


FIG. 6. Differential cross section for the reaction $K^-n \rightarrow \pi^- \Lambda$.

reaction. Figure 5 shows the $\pi^0 \Lambda$ cross section and one-half of the $\pi^- \Lambda$ cross section from various experiments.⁹⁻¹⁴ As was pointed out by Morrison,¹⁵ the variation of the cross section with the incident lab momentum is consistent with the relationship

$$\sigma(p) = c(p/p_0)^{-n},$$

where c and n are constants, p is the incident momentum in GeV/c , and p_0 is a constant also of dimensions GeV/c and is taken as $1 \text{ GeV}/c$. The least-squares-fitted values of n and c are 2.8 ± 0.1 and $3.3 \pm 0.4 \text{ mb}$, respectively.

The production angular distribution is peripherally peaked for both reactions. A small number of events are produced in the backward direction. The partial cross sections for the backward events are 9 ± 3 and $4 \pm 2 \mu\text{b}$ for reactions (1) and (2), respectively.

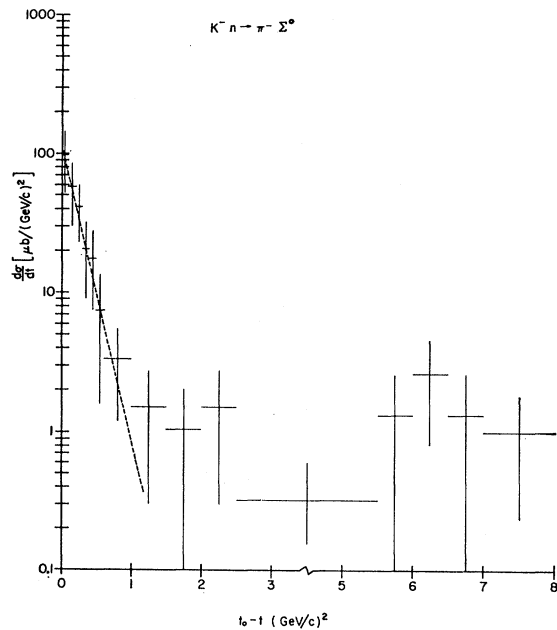


FIG. 7. Differential cross section for the reaction $K^-n \rightarrow \pi^- \Sigma^0$.

The differential cross section as a function of $t_0 - t$, where t_0 is the maximum allowable four-momentum transfer squared, are shown in Figs. 6 and 7. The peripheral peaks have been fitted to the form $d\sigma/dt$

⁹ W. Graziano and S. G. Wojcicki, *Phys. Rev.* **128**, 1868 (1962).

¹⁰ P. K. Williams, D. M. LeVine, and J. A. Koschik, University of Michigan Report, 1968 (unpublished).

¹¹ G. W. London, R. R. Rau, N. P. Samios, S. S. Yamamoto, M. Goldberg, S. Lichtman, M. Prime and J. Leitner, *Phys. Rev.* **143**, 1034 (1966).

¹² R. Barloutaud, D. N. Hoa, J. Griselin, D. W. Merrill, J. C. Scheuer, W. Hoogland, J. C. Kluyver, A. Minguzzi-Ranzi, A. M. Rossi, B. Haber, E. Hirsch, J. Goldberg, and M. Laloum, *Nucl. Phys.* **B9**, 493 (1969).

¹³ Birmingham-Glasgow-London (I.C.)-Oxford-Rutherford Collaboration, *Phys. Rev.* **152**, 1148 (1966).

¹⁴ Birmingham-Glasgow-London (I.C.)-München-Oxford-Rutherford Collaboration, *Nuovo Cimento* **53A**, 522 (1968).

¹⁵ D. R. O. Morrison, *Phys. Letters* **22**, 528 (1966).

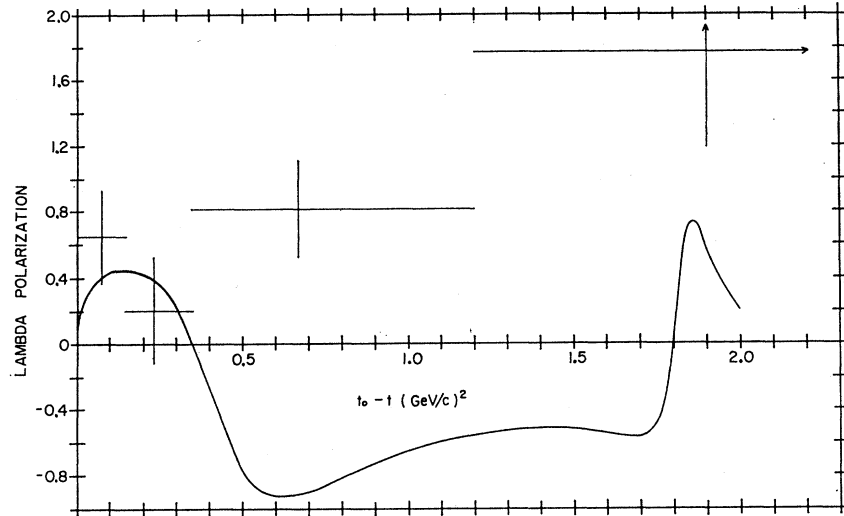


FIG. 8. Λ polarization for the reaction $K^-n \rightarrow \pi^-\Lambda$.

$= Ae^{B(t-t_0)}$. The results obtained are

$$\begin{aligned} A &= 298 \pm 73 \mu\text{b}/(\text{GeV}/c)^2, \\ B &= 4.7 \pm 1.1 (\text{GeV}/c)^{-2} \text{ for reaction (1);} \\ A &= 128 \pm 71 \mu\text{b}/(\text{GeV}/c)^2, \\ B &= 5.0 \pm 2.5 (\text{GeV}/c)^{-2} \text{ for reaction (2).} \end{aligned}$$

The experimental distributions start to deviate from this form above $t_0-t=0.5 (\text{GeV}/c)^2$. A shoulder is apparent in the differential cross section for reaction (1) at this point. These slopes are consistent with meson exchange and similar to that found in the K^-d experiment at 3 GeV/c by SABRE collaboration.¹² The SABRE experiment also shows a shoulder in the four-momentum-transfer distribution at $t_0-t \cong 0.5 (\text{GeV}/c)^2$. Experimental values of $d\sigma/dt$ for reactions (1) and (2) are given in Table III.

The polarization of the Λ is given by

$$P = \frac{3}{\alpha N} \left\{ \sum_{i=1}^N (\hat{q} \cdot \hat{n})_i \pm \left[\sum_{i=1}^N (\hat{q} \cdot \hat{n})_i^2 \right]^{1/2} \right\},$$

TABLE III. Differential cross sections for $t_0-t < 1.0 (\text{GeV}/c)^2$.

| $t_0-t (\text{GeV}/c)^2$ | | $d\sigma/dt [\mu\text{b}/(\text{GeV}/c)^2]$ | | |
|--------------------------|-----|---|----------------------------------|----------------------------------|
| From | To | $K^-n \rightarrow \Lambda\pi^-$ | $K^-n \rightarrow \Sigma^0\pi^-$ | $K^-n \rightarrow \Lambda\rho^-$ |
| 0.0 | 0.1 | 236±55 | 98±46 | } 41±11 |
| 0.1 | 0.2 | 149 32 | 58 28 | |
| 0.2 | 0.3 | 90 20 | 41 18 | } 35 10 |
| 0.3 | 0.4 | 59 15 | 20 11 | |
| 0.4 | 0.5 | 20 8 | 18 10 | } 20 7 |
| 0.5 | 0.6 | 28 10 | 7 6 | |
| 0.6 | 0.7 | 25 9 | } 3 2 | } 10 4 |
| 0.7 | 0.8 | 15 7 | | |
| 0.8 | 0.9 | 20 8 | } 9 4 | |
| 0.9 | 1.0 | 18 8 | | |

where $\alpha=0.646$ is the Λ asymmetry parameter⁷ and N is the number of events in the chosen t interval. The unit vector \hat{q} is along the decay proton direction in the hyperon c.m. system and $\hat{n} = \hat{P}_K \times \hat{P}_\pi / |\hat{P}_K \times \hat{P}_\pi|$ is a unit vector normal to the production plane. The polarization of the Λ as a function of t_0-t is shown in Fig. 8 for reaction (1). The values of the polarization is given in Table IV. No striking variation as a function of t_0-t is seen. The polarization remaining large and positive. The SABRE experiment shows similar result. Both of these are in contrast to results on hypercharge-exchange reactions at neighboring energies,¹⁶⁻¹⁸ where a change in sign is observed in the region of the dip in the differential cross-section distribution. The presence of polarization indicates that more than one Regge trajectory is exchanged. We have compared our data to a double-Regge-pole model of Reeder and Sarma¹⁹ who use $K^*(890)$ and $K^*(1420)$ exchanges to fit hypercharge-exchange reactions. The solid lines in Figs. 6 and 8 are the predictions from their model. The shape of the experimental differential cross section agrees with that predicted by the model, although it is somewhat larger

TABLE IV. Λ polarization for the reaction $K^-n \rightarrow \pi^-\Lambda$.

| t_0-t | | $\langle t_0-t \rangle_{\text{av}}$ | No. of events observed | Corrected No. of events | P | ΔP |
|---------|------|-------------------------------------|------------------------|-------------------------|------|------------|
| From | To | | | | | |
| 0.0 | 0.15 | 0.08 | 87 | 139 | 0.65 | 0.28 |
| 0.15 | 0.35 | 0.23 | 63 | 70 | 0.20 | 0.32 |
| 0.35 | 1.2 | 0.66 | 71 | 77 | 0.80 | 0.29 |
| 1.2 | 4.0 | 1.89 | 22 | 25 | 1.77 | 0.58 |
| 4.0 | 7.7 | 6.10 | 28 | 39 | 0.34 | 0.52 |

¹⁶ O. I. Dahl, L. M. Hardy, R. I. Hess, J. Kirz, D. H. Miller, and J. A. Schwartz, Phys. Rev. **163**, 1430 (1967).

¹⁷ R. R. Kofler, R. W. Hartung, and D. D. Reeder, Phys. Rev. **163**, 1479 (1967).

¹⁸ For details, see Ref. 3.

¹⁹ D. D. Reeder and K. V. L. Sarma, Phys. Rev. **172**, 1566 (1968).

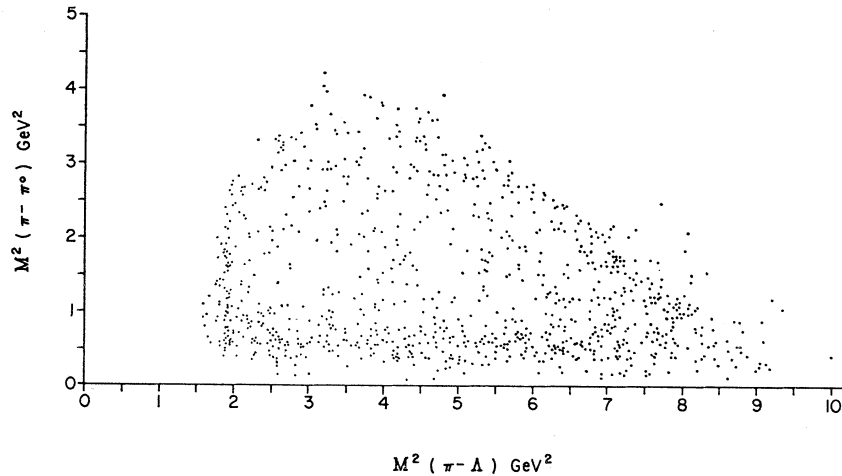


FIG. 9. Dalitz plot for the reaction $K^-n \rightarrow \pi^-\Lambda\pi^0$.

in magnitude. Our data appear to indicate that the currently adopted parameters of the $K^*(890)$ and $K^*(1420)$ trajectories are not sufficient to account for the properties of hypercharge-exchange reactions as a function of energy.

Our experimental ratio of $\sigma(\pi^-\Lambda)/\sigma(\pi^-\Sigma^0)$ is in agreement with the predicted value of 3 from $SU(3)$ and the independent quark model.²⁰ In addition, the cross section for reaction (2) is approximately half the quoted cross section²¹ for $K^-p \rightarrow \pi^-\Sigma^+$, in agreement with Ref. 20. The cross section at $t=t_0$ for reaction (1) however, is not in agreement with the predicted ratio^{20,22}

$$\left(\frac{d\sigma}{dt}\right)(K^-n \rightarrow \pi^-\Lambda) / \left(\frac{d\sigma}{dt}\right)(K^-p \rightarrow \pi^-\Sigma^+) = \frac{3}{2},$$

which we find experimentally to be 0.5 ± 0.3 .

V. FINAL STATE $p_s \pi^-\Lambda\pi^0$

A. General Features

A total sample of 904 events was accepted for analysis as being of the type $K^-n \rightarrow \pi^-\Lambda\pi^0$. The partial cross section for this reaction is $250 \pm 33 \mu\text{b}$.

A Dalitz plot is shown in Fig. 9. The presence of ρ^- is very striking. There is also evidence for the production of $\Sigma^-(1385)$ and $\Sigma^0(1385)$. Figure 10(a) shows the $\pi^-\Lambda$ effective-mass distribution. In addition to $\Sigma^-(1385)$, we see some $\Sigma^-(1610)$ production and some indications of high-mass Y^* 's. Figure 10(b) shows the $\pi^0\Lambda$ effective-mass distribution. The peak for $\Sigma^0(1385)$ looks somewhat broader. The cross sections for the $\Sigma^-(1385)$, $\Sigma^-(1610)$, and $\Sigma^0(1385)$ are estimated to be 16 ± 5 , 5 ± 3 , and $22 \pm 8 \mu\text{b}$, respectively.

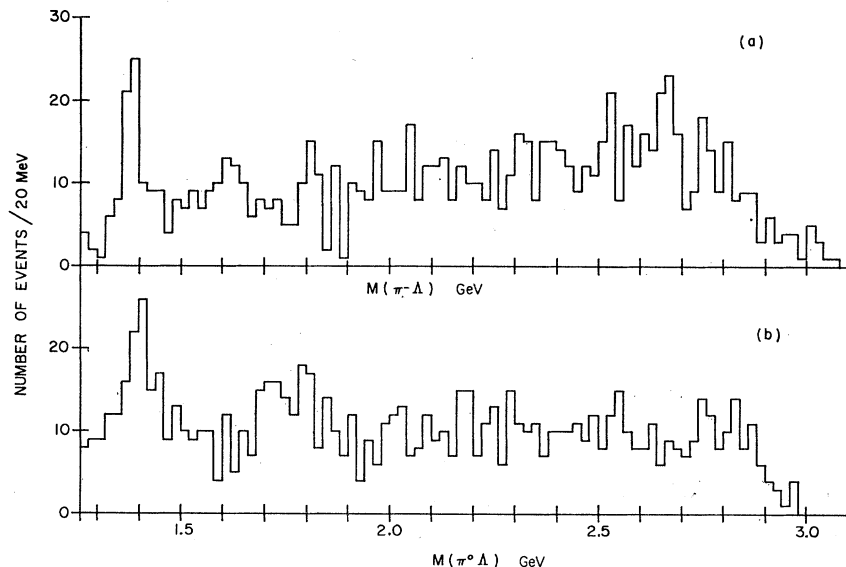


FIG. 10. $\pi\Lambda$ effective-mass distributions: (a) $\pi^-\Lambda$ system; (b) $\pi^0\Lambda$ system.

²⁰ M. P. Locher and H. Römer, Phys. Letters **23**, 496 (1966).

²¹ J. S. Loos, U. E. Kruse, and E. L. Goldwasser, Phys. Rev. **173**, 1330 (1968).

²² R. C. Arnold, Phys. Rev. **153**, 1506 (1967).

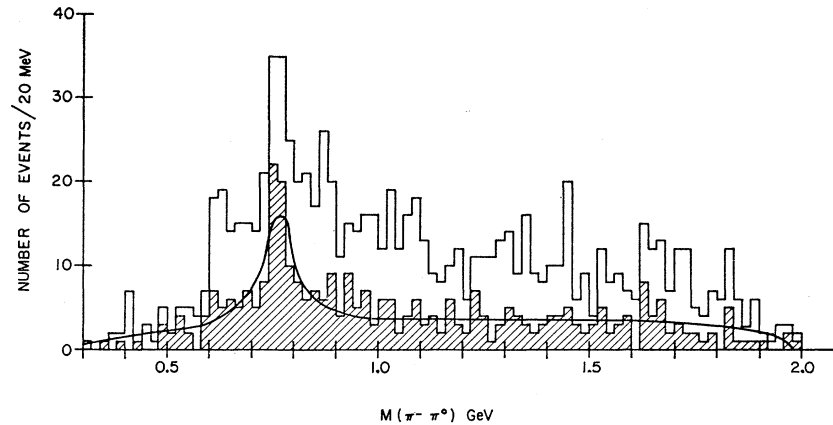
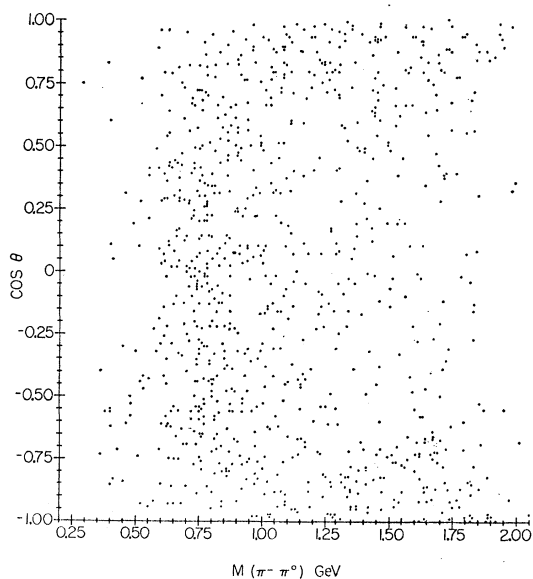
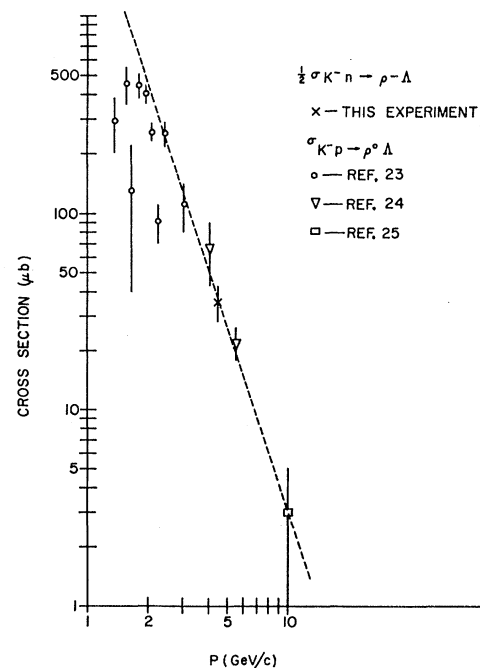
FIG. 11. $\pi^-\pi^0$ effective-mass distribution

Figure 11 shows the $\pi^-\pi^0$ effective-mass distribution. The cross-hatched area represents the events with seen spectator proton, which therefore have a better resolution. The ρ^- peak appears to be very narrow in contrast to the world average value. The solid line is the least-squares fit to the Breit-Wigner shape for the ρ^- with a background composed of normal phase space. The mass of the ρ^- obtained from the fit is 761 ± 8 MeV. The width obtained is 100 ± 20 MeV, although it is clear that the fit does not represent the data well in the ρ^- region where the width could be ~ 40 MeV. This narrow ρ^- width could be due to a fluctuation; however, it is interesting to note that the reaction $K^-n \rightarrow \rho^-\Lambda$ involves only the pure isospin-1 state, while the majority of the reactions which were used to determine the width of the ρ^- involve mixed isospin states,⁷ so that the narrow width could be a real effect. In addition, in a single-particle-exchange model we are observing the coupling

FIG. 12. Plot of $\cos\theta$ versus $\pi^-\pi^0$ effective mass.

of the K^*K to the ρ^- . Narrow widths have been reported previously particularly from $\bar{p}p$ annihilations. Figure 12 shows the plot of $\pi^-\pi^0$ effective mass versus the cosine of the decay angle θ (θ is defined as the angle between the incident K^- and the outgoing π^- in the $\pi^-\pi^0$ c.m. system). The plot shows that the $\cos\theta$ distribution changes from the shape of $\sin^2\theta$ in the ρ^- region to $\cos^2\theta$ in the higher-mass region. The region of $\sin^2\theta$ distribution is very narrow, consistent with the narrow ρ^- width. The cross section for ρ^- production is 70 ± 13 μb .

Similarly to the reactions $K^-n \rightarrow \pi^-\Lambda$ and $K^-p \rightarrow \pi^0\Lambda$, the cross section for the reaction $K^-n \rightarrow \rho^-\Lambda$ should be twice that for the reaction $K^-p \rightarrow \rho^0\Lambda$. Figure 13 shows

FIG. 13. Cross section as a function of the incident K^- momentum for the reaction $K^-N \rightarrow \rho\Lambda$.

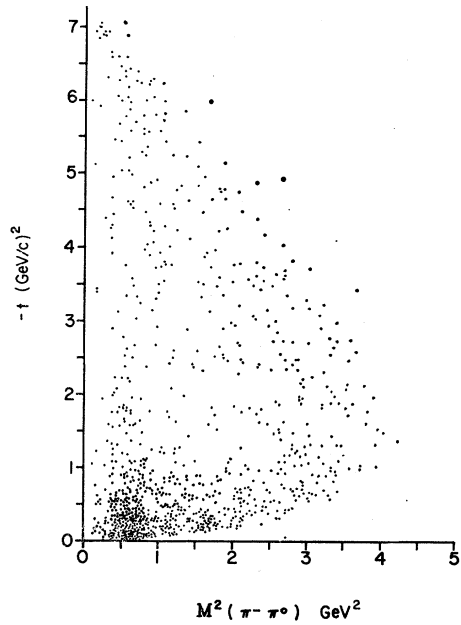


FIG. 14. Chew-Low plot for the $\pi^-\pi^0$ system in the reaction $K^-n \rightarrow \pi^-\Lambda\pi^0$.

the $\rho^0\Lambda$ cross section from previous experiments,²³⁻²⁵ together with one half of the $\rho^-\Lambda$ cross section of this analysis. The dashed line is the fit to the empirical power law for the cross section¹⁵

$$\sigma(p) = c(p/p_0)^{-n}.$$

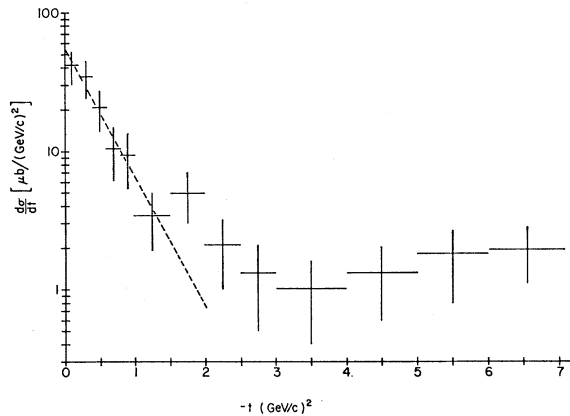


FIG. 15. Differential cross section for the reaction $K^-n \rightarrow \rho^-\Lambda$

²³ Daniel M. Siegel (Ph.D. thesis), University of California Lawrence Radiation Laboratory Report No. UCRL-18041, 1967 (unpublished), and Refs. 5, 11, 12, and 16 quoted in his thesis.

²⁴ J. Mott, R. Ammar, R. Davis, W. Kropac, D. Slate, B. Werner, S. Dagan, M. Derrick, T. Fields, J. Loken, and F. Schweingruber, Phys. Rev. **177**, 1966 (1969).

²⁵ M. Aderholz, J. Bartsch, E. Keppel, G. Kraus, R. Speth, C. Grote, J. Klugow, D. Pose, H. Schiller, M. Bardadin-Otwinowska, H. Bottcher, T. A. Byer, V. T. Cocconi, J. D. Hansen, G. Kellner, U. Kruse, J. Loskiewicz, M. Markytan, D. R. O. Morrison, S. J. Goldsack, M. E. Mermikides, N. C. Mukherjee, W. Kittel, G. Otter, P. Porth, I. Wacek, and H. Wahl, Nucl. Phys. **B5**, 606 (1968).

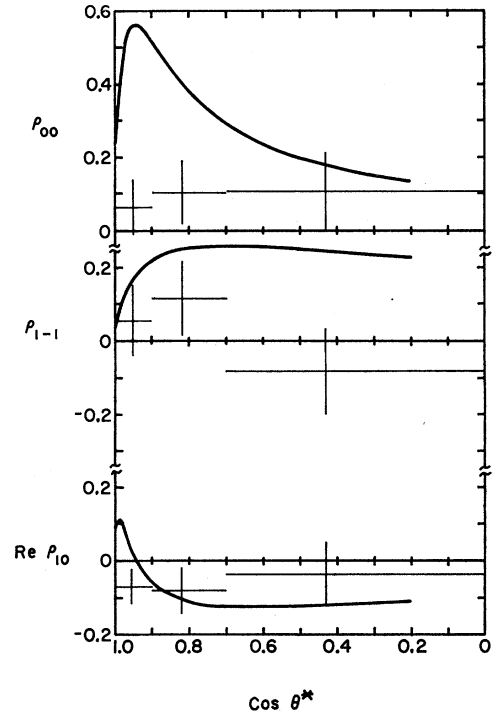


FIG. 16. Density matrix element for ρ^- in the reaction $K^-n \rightarrow \rho^-\Lambda$.

The notation is the same as in reaction $K^-n \rightarrow \Lambda\pi^-$. The values of n and c are 3.1 ± 0.3 and 4.0 ± 1.2 mb, respectively. Since both reactions $KN \rightarrow \pi\Lambda$ and $KN \rightarrow \rho\Lambda$ proceed by exchange of strange mesons, the values of n are expected to be the same in a simple Regge-pole model.¹⁵ Our values are consistent with equality within errors.

A Chew-Low plot for the $\pi^-\pi^0$ system is shown in

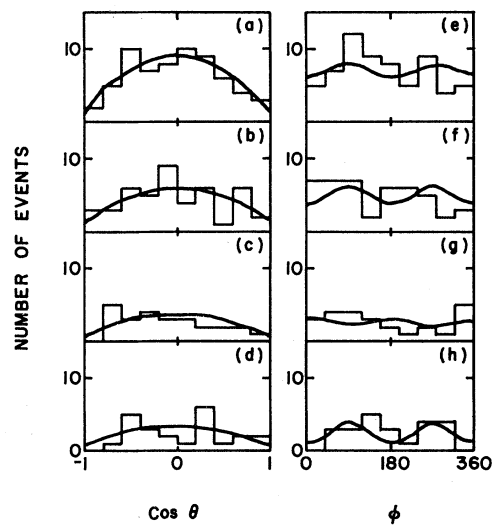


FIG. 17. $\cos\theta$ and ϕ distributions for ρ^- events: (a), (c) $1.0 \geq \cos\theta^* > 0.9$; (b), (f) $0.9 \geq \cos\theta^* > 0.7$; (c), (g) $0.7 \geq \cos\theta^* > 0.0$; (d), (h) $0.0 \geq \cos\theta^* \geq -1.0$.

TABLE V. Density matrix element for ρ^- in the reaction $K^-n \rightarrow \rho^- \Lambda$.

| $\cos\theta^*$ | | $\langle \cos\theta^* \rangle_{av}$ | No. of events | Corrected No. of events | ρ_{00} | $\Delta\rho_{00}$ | ρ_{1-1} | $\Delta\rho_{1-1}$ | $\text{Re}\rho_{10}$ | $\Delta\text{Re}\rho_{10}$ |
|----------------|------|-------------------------------------|---------------|-------------------------|-------------|-------------------|--------------|--------------------|----------------------|----------------------------|
| From | To | | | | | | | | | |
| 1.0 | 0.9 | 0.95 | 64 | 73 | 0.067 | 0.073 | 0.058 | 0.093 | -0.069 | 0.047 |
| 0.9 | 0.7 | 0.82 | 45 | 48 | 0.103 | 0.088 | 0.116 | 0.100 | -0.079 | 0.061 |
| 0.7 | 0.0 | 0.44 | 25 | 27 | 0.107 | 0.102 | -0.082 | 0.118 | -0.035 | 0.088 |
| 0.0 | -1.0 | -0.66 | 23 | 31 | 0.076 | 0.096 | 0.286 | 0.128 | 0.060 | 0.065 |

Fig. 14. It shows that the reaction $K^-n \rightarrow \rho^- \Lambda$ occurs mainly at small values of $-t$, the four-momentum transfer squared to the hyperon. Even outside the region of ρ^- , one observes a general concentration of events on the lower $-t$ region. This illustrates that the reaction $K^-n \rightarrow \pi^- \Lambda \pi^0$ is dominated by peripheral processes at this energy.

B. Production and Decay of the ρ^-

Events with the $\pi^- \pi^0$ effective mass squared lying between 0.49 and 0.68 GeV^2 were taken as being representative of the ρ^- production and decay. Taking into account the background, it was estimated that about 27% of these events did not correspond to the ρ^- production.

The production angular distribution of the $\pi^- \pi^0$ system in the $\pi^- \Lambda \pi^0$ c.m. system for these events is shown in Fig. 15 and is given in Table III as a function of $-t$. It shows a strong forward peak, a characteristic feature of meson exchange, and a much smaller backward peak which could arise from baryon exchange. The peripheral peak has been fitted to the form $d\sigma/dt = Ae^{Bt}$. The results obtained are $A = 57 \pm 17 \mu\text{b}/(\text{GeV}/c)^2$, and $B = 2.2 \pm 0.8 (\text{GeV}/c)^{-2}$.

In the context of the peripheral model, K , $K^*(890)$, $K^*(1420)$, and other not so well-established resonances, such as $K^*(1250)$ can participate in the reaction $K^-n \rightarrow \rho^- \Lambda$. In order to understand the production mechanism of this reaction, it is important to find out experimentally which meson or mesons are really exchanged.

The ρ^- decay distribution can be written in terms of its spin space density matrix elements $\rho_{mm'}$ as²⁶

$$W(\theta, \varphi) = (3/4\pi)(\rho_{00} \cos^2\theta + \rho_{11} \sin^2\theta - \rho_{1-1} \sin^2\theta \cos 2\varphi - \sqrt{2} \text{Re}\rho_{10} \sin 2\theta \cos \varphi),$$

with the trace condition that $\rho_{00} = 1 - 2\rho_{11}$. The angles θ and φ are the polar and azimuthal angles of the decay π^- in the ρ^- rest system, the z axis being taken as the direction of the incident K^- , the y axis as the direction of the normal to the production plane.

The method of moments²⁷ was used in the determination of the density matrix elements. The results are shown in Fig. 16 and are given in Table V.

²⁶ K. Gottfried and J. D. Jackson, *Nuovo Cimento* **33**, 309 (1964).

²⁷ See, for example, N. Schmitz, in Proceedings of the 1965 Easter School for Physicists at Bad Kreuznach, CERN Report No. 65-24, Vol. I, p. 26 (unpublished).

Integration of the function $W(\theta, \varphi)$ gives the distribution expected in θ and φ :

$$W(\theta) = \frac{3}{4}[(1 - \rho_{00}) + (3\rho_{00} - 1) \cos^2\theta],$$

$$W(\varphi) = (1/2\pi)[(1 + 2\rho_{1-1}) - 4\rho_{1-1} \cos^2\varphi].$$

Figure 17 shows the $\cos\theta$ and φ distribution for successive intervals of $\cos\theta^*$ (θ^* is the production angle between the incident K^- to the outgoing ρ^- in the total c.m. system). The solid lines are the expected distributions with the experimental density matrix elements determined by the method of moments.

Without the effect of absorption, the smallness of ρ_{00} together with the $\sin^2\theta$ distribution in Fig. 17 indicate that vector or higher-spin exchange dominates the production process. Since $K^*(890)$ is the lightest candidate, the exchange of this resonance was assumed and predictions of the one-meson-exchange model with absorption (OMEA)^{28,29} were made. The solid lines in Fig. 16 are the OMEA predictions. The discrepancy between our results, especially ρ_{00} , and OMEA is quite apparent. This discrepancy indicates that the assumed $K^*(890)$ dominant is incorrect. Another investigation given below also support this conclusion.

If the dominant mechanism for the production of ρ^- is the exchange of a single set of quantum numbers (i.e., a single Regge trajectory), the quantity $|\rho_{1-1}|/\rho_{11}$ has an upper and lower bound³⁰

$$\frac{x^2 - 1}{x^2 + 1} \leq \frac{|\rho_{1-1}|}{\rho_{11}} \leq 1,$$

where x is the cosine of the scattering angle in the crossed channel. The plot of $|\rho_{1-1}|/\rho_{11}$ as a function of $\cos\theta^*$ is shown in Fig. 18. The solid curve is the lower bound $(x^2 - 1)/(x^2 + 1)$. It shows that $|\rho_{1-1}|/\rho_{11}$ fails to satisfy the lower bound. The failure indicates that more than one exchange contributes.

C. Production of the $\Sigma^-(1385)$ and $\Sigma^0(1385)$

Events with the $\pi\Lambda$ effective mass lying between 1.33 and 1.45 GeV were taken as being representative of the $\Sigma(1385)$ production. Taking the background into account, it was estimated that about 49 and 28% of

²⁸ J. D. Jackson, *Rev. Mod. Phys.* **37**, 484 (1965); J. D. Jackson, J. T. Donohue, K. Gottfried, R. Keyser, and B. E. Y. Svensson, *Phys. Rev.* **139**, B428 (1965).

²⁹ The predictions were computed by using a program by R. Keyser, CERN Report No. DD/CO/66/3 (unpublished).

³⁰ G. A. Ringland and R. L. Thews, *Phys. Rev.* **170**, 1569 (1968).

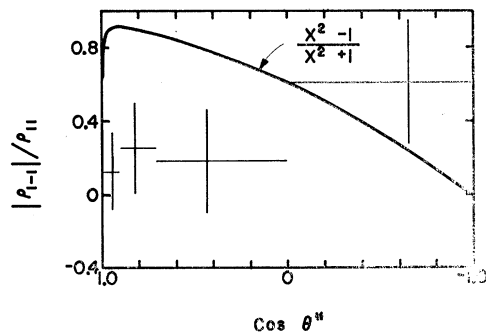


FIG. 18. Comparison of the density matrix element to the prediction for a single Regge-trajectory exchange.

these events did not correspond to $\Sigma^0(1385)$ and $\Sigma^-(1385)$ production, respectively.

The momentum transfer distribution for these events is shown in Fig. 19. It shows a strong forward peak, a characteristic feature of meson exchange.

VI. FINAL STATE $p_s \pi^- \Lambda + \text{NEUTRALS}$

A. General Features

A total sample of 2778 events was accepted as belonging to reaction (4). The missing-mass and effective-mass-squared distribution of all possible combinations of particles of this final state was plotted in Figs. 20 and 21. They show η and strong $\Sigma^-(1385)$ produc-

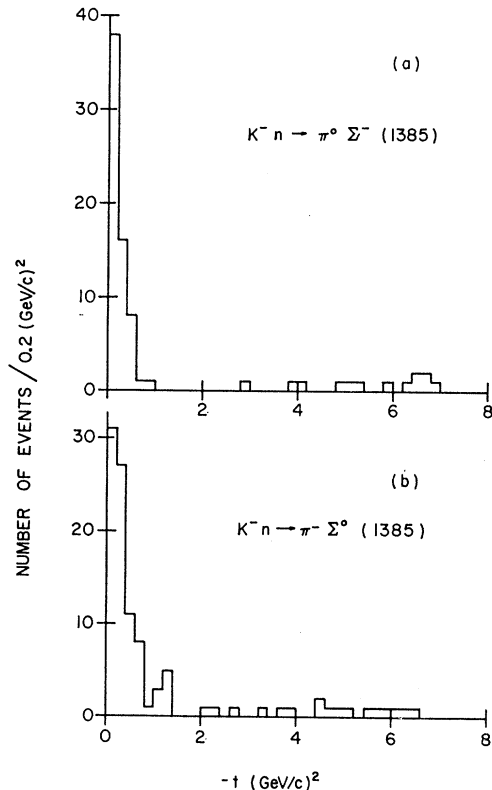


FIG. 19. Momentum transfer distribution: (a) $K^- n \rightarrow \Sigma^-(1385)\pi^0$; (b) $K^- n \rightarrow \Sigma^0(1385)\pi^-$.

tion. In addition, there is some evidence for the production of $\Sigma^-(1610)$, and $\Sigma^-(1765)$. The production of the η is more clearly seen when events with unseen spectator proton and with the four-momentum transfer squared from K^- to the π^-MM system greater than 1 $(\text{GeV}/c)^2$ were excluded from the sample. This distribution is shown in Fig. 20(b).

The enhancements for the $\Sigma^-(1610)$ and $\Sigma^-(1765)$ are not improved by taking any cut in the four-momentum transfer to the $\pi^- \Lambda$ system. Because of the large background accompanying with these enhancements, no further analysis will be attempted for these states.

B. Reaction $K^- n \rightarrow \pi^- \Lambda \eta$

Events with the missing mass squared lay between $0.23 < MM^2 < 0.36 \text{ GeV}^2$ were taken as being representative of the production of the η . The 282 events selected have a background from non- η events of approximately 50%. The partial cross section for this reaction is $56 \pm 15 \mu\text{b}$. Figure 22(a) shows the $\pi^- \eta$ effective mass distribution for these events. A rather broad enhancement can be seen near 1 GeV^2 . The enhancement is more striking if events with four-momentum transfer squared from K^- to π^-MM greater than 1 $(\text{GeV}/c)^2$ and events with the $\pi^- \Lambda$ effective mass falling in the $\Sigma^-(1385)$ band were excluded. This is shown in Fig. 22(b).

This enhancement, which we have reported previously, we interpret as production of the $\pi_N(980)$ reported recently,³¹⁻³³ and is summarized in Sec. VI C. The cross section for this state is $15 \pm 3 \mu\text{b}$.

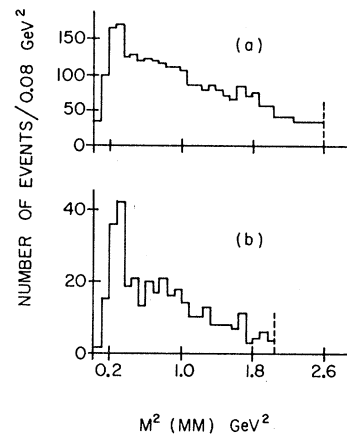


FIG. 20. Missing-mass distribution for $K^- n \rightarrow \pi^- \Lambda$ neutrals: (a) Total sample; (b) events with seen proton spectator and the four-momentum transfer squared from the incident K^- to the π^-MM system less than 1 $(\text{GeV}/c)^2$.

³¹ R. Ammar, R. Davis, W. Kropac, J. Mott, D. Slate, B. Werner, M. Derrick, T. Fields, and F. Schweingruber, *Phys. Rev. Letters* **21**, 1832 (1968).

³² N. P. Samios, in *Proceedings of the Informal Meeting on Experimental Meson Spectroscopy, Philadelphia, Pennsylvania*, (W. A. Benjamin, Inc., New York, 1968); V. Barnes, P. Dornan, P. Guidoni, N. Samios, M. Goldberg, and J. Leitner, presentation in *Proceedings of the Fourteenth International Conference on High Energy Physics, Vienna, 1968* (CERN, Geneva, 1968).

³³ C. Defoix, P. Rivet, J. Slaud, B. Conforto, M. Widgoff and F. Shively, *Phys. Letters* **28B**, 353 (1968).

In addition to the observation of the $\pi_N(980)$ state, there are also strong production of $\Sigma^-(1385)$ and some indications of the production of $\Sigma^-(1610)$ and $\Sigma^-(2250)$ as can be seen in Fig. 22(d). The cross sections for $\Sigma^-(1385)$ and $\Sigma^-(1610)$ are estimated to be 13 ± 4 and $5 \pm 3 \mu\text{b}$, respectively. The background under the $\Sigma^-(2250)$ is so high that no cross-section estimation is attempted.

C. Production and Decay of the $\pi_N(980)$

In Fig. 23 we show the Chew-Low plot for the reaction $K^-n \rightarrow \pi^- \eta \Lambda$ with events corresponding to $\Sigma^-(1385)$ production removed. A marked clustering at small four-momentum transfer squared (from the incident K^- to the π^- system) can be seen in the region of the en-

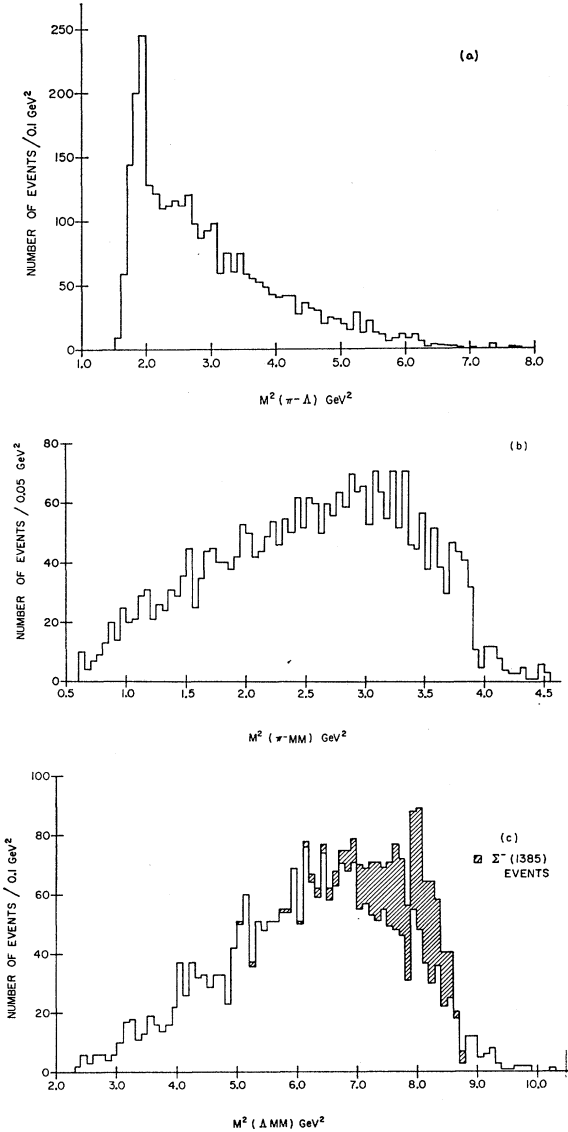


FIG. 21. Effective-mass distribution for reaction (4): (a) $M^2(\pi^-\Lambda)$; (b) $M^2(\pi^-MM)$; (c) $M^2(\Lambda MM)$.

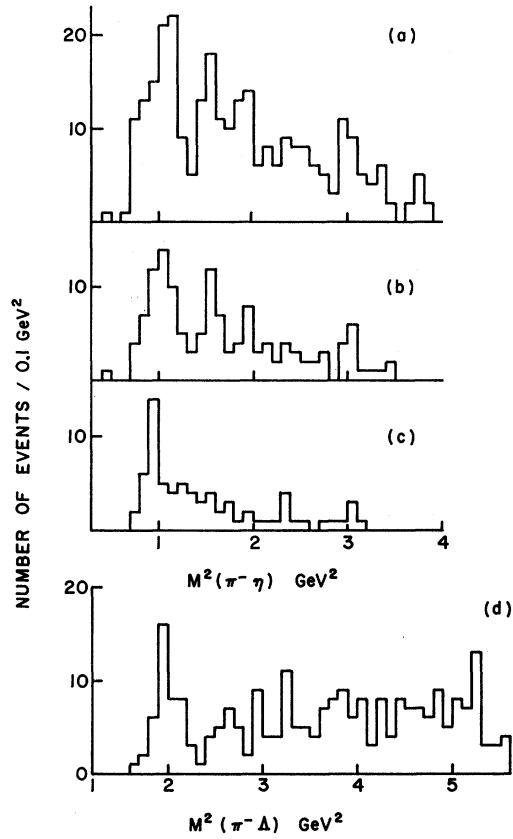


FIG. 22. Effective-mass distribution for the reaction $K^-n \rightarrow \pi^-\Lambda\eta$: (a) $M^2(\pi^-\eta)$, total events; (b) $M^2(\pi^-\eta)$, events with $-t_{K \rightarrow \pi-MM} < 1$ (GeV/c)² and no $\Sigma^-(1385)$; (c) fitted $\pi^-\eta$ mass distribution with $-t < 1$ (GeV/c)² and no $\Sigma^-(1385)$; (d) $M^2(\pi^-\eta)$

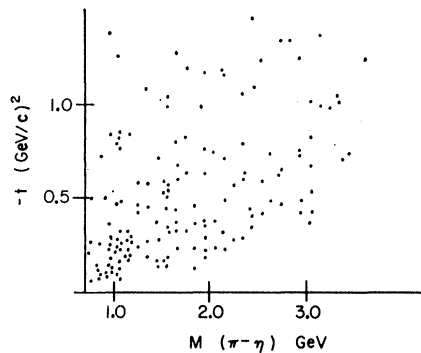


FIG. 23. Chew-Low plot for the reaction $K^-n \rightarrow \Lambda\pi^-\eta$ with events corresponding to $\Sigma^-(1385)$ production removed.

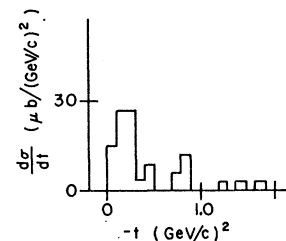


FIG. 24. Differential cross section for the reaction $K^-n \rightarrow \pi_N^-(980)\Lambda$.

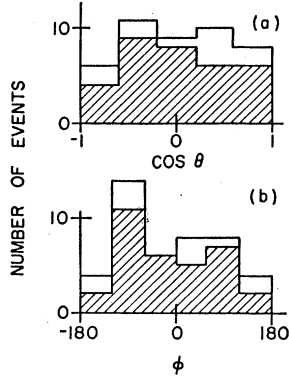


FIG. 25. Decay angular distribution for $\pi_N(980)$ events; the shaded area is for events with $-t < 1$ (GeV/c)²: (a) $\cos\theta$ distribution; (b) Treiman Yang angle.

hancement near 1 GeV^2 . The clustering of events at low four-momentum transfer squared indicate that the resonance is produced by single meson exchange. This enhancement appears to be only produced in the region where the missing neutrals have a mass consistent with the η .⁴

The best estimate of the mass and width come from the two prong plus V events which fit the hypothesis $K^-d \rightarrow \bar{p}_s \pi^- \Lambda \eta$. Figure 22(c) shows the $\pi^- \eta$ effective-mass distribution for those events with $-t < 1$ (GeV/c)² and with the $\Sigma^-(1385)$ removed. We obtain a mass of 0.98 ± 0.01 GeV and a width of 60 ± 30 MeV .

The differential cross section for the $\pi_N(980)$ events is shown in Fig. 24 and is consistent with a peripheral production mechanism. The decay angular distributions in the $\pi^- \eta$ rest system are shown in Fig. 25. Both $\cos\theta$ and φ distributions favor isotropy, the $\cos\theta$ distribution having a probability of 75% of being isotropic. The production and decay definitely establish $I=1$, and the width and decay distributions are consistent with a strong decay of a $J^P=0^+$ state.

We have looked for the $\pi_N(980)$ decay into $\pi^- \eta$ ($\eta \rightarrow \pi^- \pi^+ \pi^0$) in the final state $\Lambda \pi^+ \pi^- \pi^0$. It appears that the correct number of events exist in the 980-MeV region (in Fig. 26). A recent paper by Crennell *et al.*³⁴ concludes that this resonance is, in fact, a kinematic

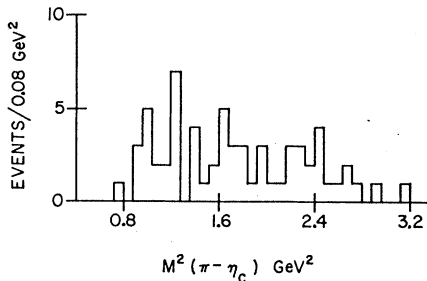


FIG. 26. $\pi^- \eta_c$ effective-mass distribution for the reaction $K^- n \rightarrow \pi^- \Lambda \eta_c \pi^+ \pi^- \pi^0$.

³⁴ D. J. Crennell, U. Karshon, K. W. Lai, J. S. O'Neill, J. M. Scarr, P. Baumel, R. M. Lea, T. G. Schumann, and E. M. Urwater, Phys. Rev. Letters 22, 1398 (1969).

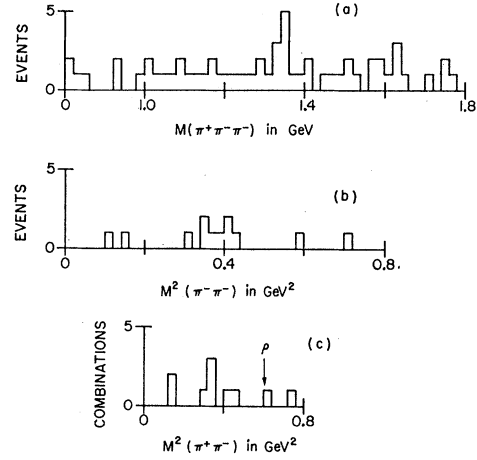


FIG. 27. Effective-mass distribution for the reaction $K^- n \rightarrow \Lambda \pi^+ \pi^- \pi^-$: (a) $\pi^+ \pi^- \pi^-$ mass distribution with $0.22 < M^2(\pi^+ \pi^-) < 0.4$ GeV^2 ; (b) $\pi^- \pi^-$ mass distribution with $0.98 < M(\pi^+ \pi^-) < 1.06$ GeV ; (c) $\pi^+ \pi^-$ mass distribution with $0.98 < M(\pi^+ \pi^-) < 1.06$ GeV and $0.22 < M^2(\pi^- \pi^-) < 0.4$ GeV^2 .

effect coming from the reaction $K^- n \rightarrow \Lambda \pi^- \pi^0 \pi^0$ (particularly $\Delta \rho^- \pi^0$ final states, the $\pi^0 \pi^0$ system having the kinematic property of being peaked in the η region. In a study of the reaction $K^- d \rightarrow \bar{p}_s \Lambda \pi^+ \pi^- \pi^-$ (453 events), we find that our data are somewhat different from those of Ref. 34, although statistically weaker. Using the same criteria as those used in Figs. 2(b), 2(d), and 2(e) in Ref. 34, we plot $M(\pi^+ \pi^- \pi^-)$, $M^2(\pi^- \pi^-)$, and $M^2(\pi^+ \pi^-)$ distributions in Fig. 27. In Fig. 27(a) we do not observe an enhancement at ~ 1.0 GeV , in contrast to the result of Ref. 34.³⁵ In Fig. 27(c) no marked ρ^0 signal is observed, again in contrast to the

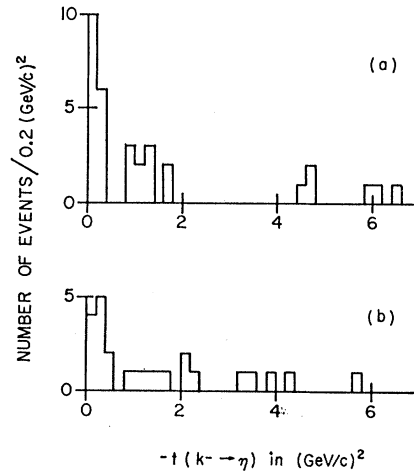


FIG. 28. Momentum transfer distribution: (a) $K^- n \rightarrow \Sigma^-(1385) \eta$; (b) $K^- n \rightarrow \Sigma^-(1610) \eta$.

³⁵ If we examine the $\pi^+ \pi^- \pi^-$ mass spectrum in the 0.98- GeV region with the four-momentum transfer squared less than 1.0 (GeV/c)², we find no enhancement. In fact, there are 4 ± 2 events above background as compared to 24 ± 5 events expected if the $\pi_N(980)$ were really a $\rho \pi$ resonance.

result of Ref. 34. Thus it does not appear that the effect at 980 MeV observed in our data is wholly kinematic in origin. Additional evidence against this type of kinematical interpretation has been given recently.^{36,37}

D. Final States $\Sigma^-(1385)\eta$ and $\Sigma^-(1610)\eta$

Events with the π^-A effective mass squared lying between 1.80 and 2.10 GeV^2 were taken as being representative of the $\Sigma^-(1385)$ production. Taking the background into account, it was estimated that about 25% of these events did not correspond to $\Sigma^-(1385)$ production. The four-momentum-transfer distribution is shown in Fig. 28(a). The production process appears to be peripheral.

³⁶ V. E. Barnes, S. U. Chung, R. L. Eisner, E. Flaminio, P. Guidoni, J. B. Kinson, N. P. Samios, D. Bassano, M. Goldberg, and K. Jaeger, *Phys. Rev. Letters* **23**, 610 (1969).

³⁷ J. Mott, paper presented at the meeting of the division of particles and fields, Boulder, Colo. 1969 (unpublished).

Events with the π^-A effective mass squared lying between 2.4 and 2.8 GeV^2 were taken as being representative of the $\Sigma^-(1610)$ production. Taking into account the background, it was estimated that about 60% of these events did not correspond to $\Sigma^-(1610)$ production. The four-momentum transfer distribution is shown in Fig. 28(b). This reaction is not as peripheral as the reaction $K^-n \rightarrow \eta\Sigma^-(1385)$.

ACKNOWLEDGMENTS

We would like to express our gratitude to the operating personnel of the bubble chamber and the staff of Argonne National Laboratory, particularly Dr. M. Derrick, Dr. L. Voyvodic, and Dr. F. Schweingruber, for their help. We would also like to thank the scanning and measuring crew for their cooperation and care in the film analysis.

Coherent Production of the $K^-\pi^+\pi^-$ System in K^-d Interactions at 5.5 GeV/c^\dagger

B. WERNER,* R. AMMAR,† R. E. P. DAVIS, W. KROPAC,‡ AND H. YARGER†

Northwestern University, Evanston, Illinois 60201

AND

Y. CHO, M. DERRICK, B. MUSGRAVE, J. J. PHELAN,§ AND T. P. WANGLER

Argonne National Laboratory, Argonne, Illinois 60439

(Received 7 July 1969)

K^-d interactions were studied at an incident momentum of 5.5 GeV/c in a 5-eV/ μb exposure of the 30-in. deuterium bubble chamber at the Argonne Zero-Gradient Synchrotron. The dominant feature of the reaction $K^-d \rightarrow K^-\pi^+\pi^-d$ is $\bar{K}^*(890)$ production, although the low-mass enhancement, usually referred to as d^* , is also prominent in the $d\pi^-$ mass spectrum. The low momentum transfer to the deuteron imposed by coherent production strongly favors a $K\pi\pi$ mass in the region of the Q enhancement. As is usually observed, the production and decay characteristics of the $K\pi\pi$ system are generally compatible with a 1^+ spin-parity assignment. A study of the $K^-\pi^+$ system reveals an s -wave- p -wave interference similar to that observed in $K\pi$ scattering. The data are compared with the predictions of a double-Regge-pole model.

I. INTRODUCTION

THE results reported in this paper were obtained from a 370 000-picture exposure of the 30-in. deuterium bubble chamber to an electrostatically separated, high-purity beam¹ of 5.5- GeV/c negative

kaons produced at the Argonne Zero-Gradient Synchrotron (ZGS). The experimental arrangement was identical to that used in a previous study of K^-p interactions at this energy.² We have analyzed those four-prong events with at least one stopping positive track which is either a proton or a deuteron and studied the reaction

$$K^-d \rightarrow K^-\pi^+\pi^-d. \quad (1.1)$$

Coherent $K\pi\pi$ production has been studied at other energies using both incident K^+ and K^- mesons.³⁻⁶ At 5.5 GeV/c the kinematics of coherent production

† Work supported by U. S. Atomic Energy Commission and the National Science Foundation.

* This work forms part of a dissertation to be submitted to the Department of Physics, Northwestern University, in partial fulfillment of the requirements for the Ph.D. degree.

† Present address: Department of Physics, University of Kansas, Lawrence, Kan. 66044.

§ Now at the Rutherford Laboratory, Chilton, Didcot, Berkshire, England.

¹ T. H. Fields *et al.*, Argonne National Laboratory Report No. THF/ELG/UEK-1, 1961 (unpublished); R. Ammar *et al.*, in Proceedings of the 1966 International Conference on Instrumentation for High-Energy Physics, Stanford-USAEC Report No. 660918, p. 620 (unpublished).

² F. Schweingruber *et al.*, *Phys. Rev.* **166**, 1317 (1968).

³ I. Butterworth *et al.*, *Phys. Rev. Letters* **15**, 500 (1965).

⁴ D. Denegri *et al.*, *Phys. Rev. Letters* **20**, 1194 (1968).

⁵ W. Hoogland *et al.*, *Nucl. Phys.* **B11**, 309 (1969).

⁶ K. Buchner *et al.*, *Nucl. Phys.* **B9**, 286 (1969).